Tectonophysics 722 (2018) 277–285

Contents lists available at ScienceDirect

Tectonophysics

journal homepage: www.elsevier.com/locate/tecto

West-directed thrusting south of the eastern Himalayan syntaxis indicates clockwise crustal flow at the indenter corner during the India-Asia collision

Peter J. Haproff[a,*], Andrew V. Zuza[a,b], An Yin[a]

[a] Department of Earth, Planetary, and Space Sciences, University of California, Los Angeles, CA 90095-156702, USA
[b] Nevada Bureau of Mines and Geology, University of Nevada, Reno, NV 89557, USA

ARTICLE INFO

Keywords:
Himalaya
Tibet
Eastern Himalayan syntaxis
Extrusion tectonics
Crustal flow
Thrust tectonics

ABSTRACT

Whether continental deformation is accommodated by microplate motion or continuum flow is a central issue regarding the nature of Cenozoic deformation surrounding the eastern Himalayan syntaxis. The microplate model predicts southeastward extrusion of rigid blocks along widely-spaced strike-slip faults, whereas the crustal-flow model requires clockwise crustal rotation along closely-spaced, semi-circular right-slip faults around the eastern Himalayan syntaxis. Although global positioning system (GPS) data support the crustal-flow model, the surface velocity field provides no information on the evolution of the India-Asia orogenic system at million-year scales. In this work, we present the results of systematic geologic mapping across the northernmost segment of the Indo-Burma Ranges, located directly southeast of the eastern Himalayan syntaxis. Early research inferred the area to have experienced either right-slip faulting accommodating northward indentation of India or thrusting due to the eastward continuation of the Himalayan orogen in the Cenozoic. Our mapping supports the presence of dip-slip thrust faults, rather than strike-slip faults. Specifically, the northern Indo-Burma Ranges exposes south- to west-directed ductile thrust shear zones in the hinterland and brittle fault zones in the foreland. The trends of ductile stretching lineations within thrust shear zones and thrust sheets rotate clockwise from the northeast direction in the northern part of the study area to the east direction in the southern part of the study area. This clockwise deflection pattern of lineations around the eastern Himalayan syntaxis mirrors the clockwise crustal-rotation pattern as suggested by the crustal-flow model and contemporary GPS velocity field. However, our finding is inconsistent with discrete strike-slip deformation in the area and the microplate model.

1. Introduction

Fundamental questions in studies of continental tectonics are whether continental deformation is accommodated by the interaction of microplate motion (McKenzie, 1972; Avouac and Tapponnier, 1993) or continuum flow (England and McKenzie, 1982; England and Houseman, 1986) and how this interaction might have impacted regional topographic evolution and climate changes (e.g., Ding et al., 2014, 2017). The question of how the continental lithosphere deforms is manifested in the ongoing debate about the nature of Cenozoic tectonic deformation across Southeast Asia surrounding the eastern Himalayan syntaxis (Fig. 1). The microplate model predicts southeastward translation of rigid blocks such as Indochina along relatively linear conjugate strike-slip faults (Tapponnier et al., 1986; Leloup et al., 2001; Akciz et al., 2008), whereas the crustal-flow model requires the development of closely spaced, semi-circular, thrust and right-slip faults surrounding the eastern Himalayan syntaxis to accommodate clockwise crustal rotation (Cobbold and Davy, 1988; Royden et al., 1997; Wang et al., 1998). Although the results of several global positioning system (GPS) velocity-field studies (Zhang et al., 2004; Gan et al., 2007; Maurin et al., 2010) and modeling efforts (e.g., Chang et al., 2015) support the crustal flow model, the surface velocity field provides no information on the long-term tectonic development of the India-Asia collision zone. For example, it is possible that microplate motion as expressed by extrusion tectonics occurred first followed by crustal flow around the eastern Himalayan syntaxis (e.g., Kornfeld et al., 2014). Such a two-phase scenario would require early formation of widely spaced, linear strike-slip faulting that was followed by younger closely-spaced and curved strike-slip faults (e.g., Wang and Burchfiel, 1997; Royden et al., 1997).

A key test of these two competing models is whether upper plate continental deformation directly south of the eastern Himalayan syntaxis across the northernmost Indo-Burma Ranges is accommodated by right-slip faulting (Fig. 2A) (Mitchell, 1993) or west-directed thrusting (Fig. 2B) (Gururajan and Choudhuri, 2003; Misra, 2009). In this study, we present the results of systematic geologic mapping in this key area

* Corresponding author.
E-mail addresses: peterhaproff@ucla.edu, peterhaproff@gmail.com (P.J. Haproff).

https://doi.org/10.1016/j.tecto.2017.11.001
Received 30 August 2017; Received in revised form 27 October 2017; Accepted 2 November 2017
Available online 09 November 2017
0040-1951/

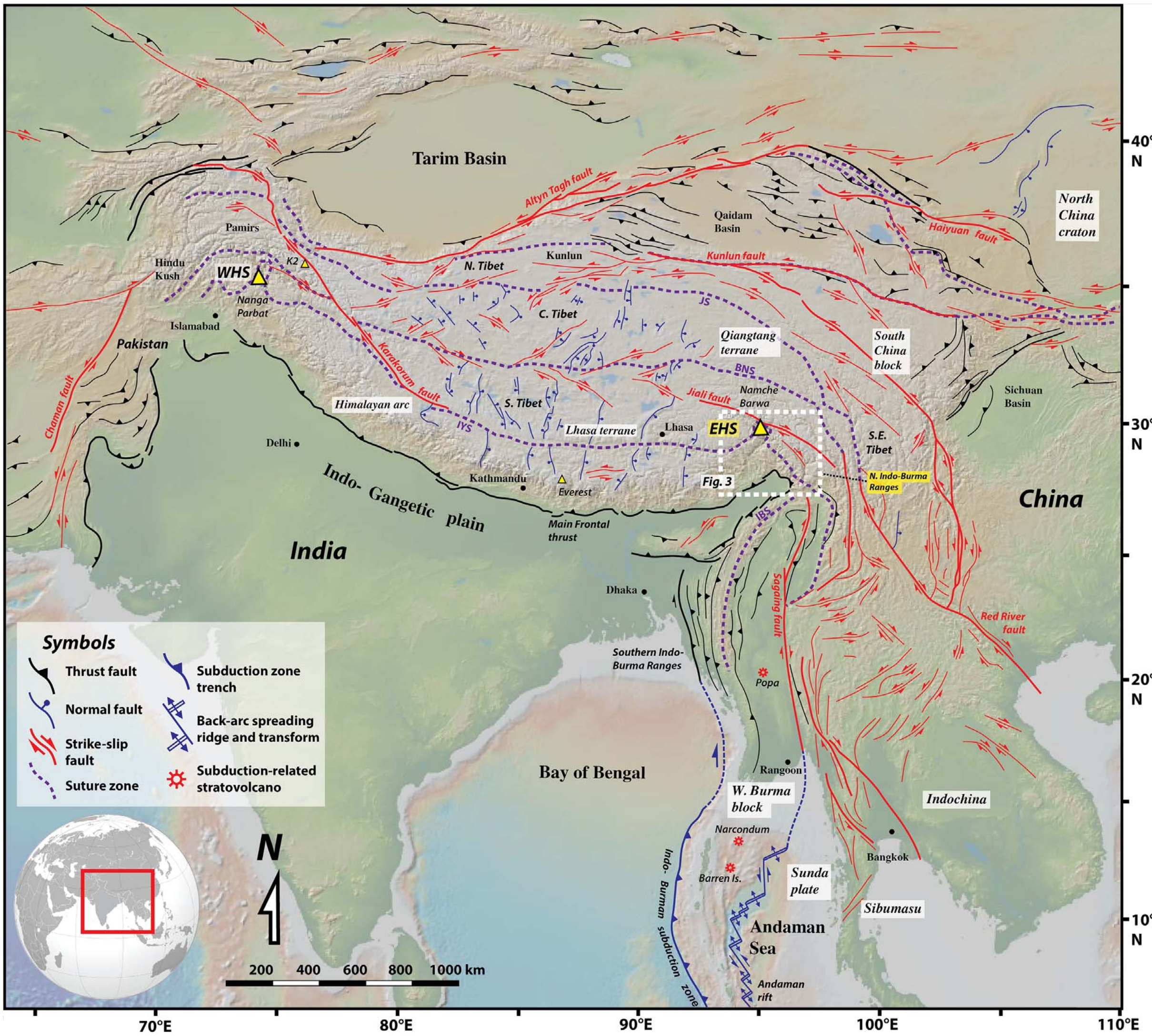

Fig. 1. Tectonic map of the Indo-Asian collision zone modified from Taylor and Yin (2009). The northern Indo-Burma Ranges are shown within the white box (Fig. 3). The digital elevation map was acquired using *geomapapp.com* (Ryan et al., 2009). The Earth index map was acquired through Generic Mapping Tools (*gmt.soest.hawaii.edu*). Abbreviations: BNS: Bangong-Nujiang suture, EHS: eastern Himalayan syntaxis, IYS: Indus-Yarlung suture, JS: Jinsha suture, WHS: western Himalayan syntaxis.

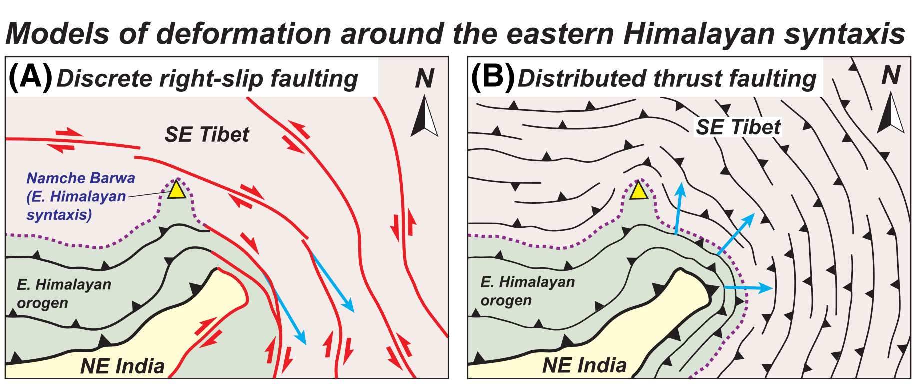

Fig. 2. End-member models for upper plate continental deformation surrounding the eastern Himalayan syntaxis during the Cenozoic India-Asia collision, (A) discrete right-slip faulting versus (B) distributed thrust faulting. Predictions of stretching lineation orientations are shown as blue arrows.

(Figs. 1 and 3). Our work shows that the dominant structures across a ~100-km wide deformation zone are southwest-directed thrusts that have accommodated > 10′s km of crustal shortening during the Cenozoic. This finding is consistent with the continuum flow models of England and Houseman (1986), Cobbold and Davy (1988), and Royden et al. (1997) that predict that the overriding Asian plate during the India-Asia collision is highly mobile and capable of flowing along the maximum gradient of the gravitational potential energy stored in the thickened Tibetan lithosphere. To focus on the results of our geologic mapping, we provide only a general overview of the lithologic descriptions and timing constraints for the rock units and deformation events, as these materials will be presented in separate papers.

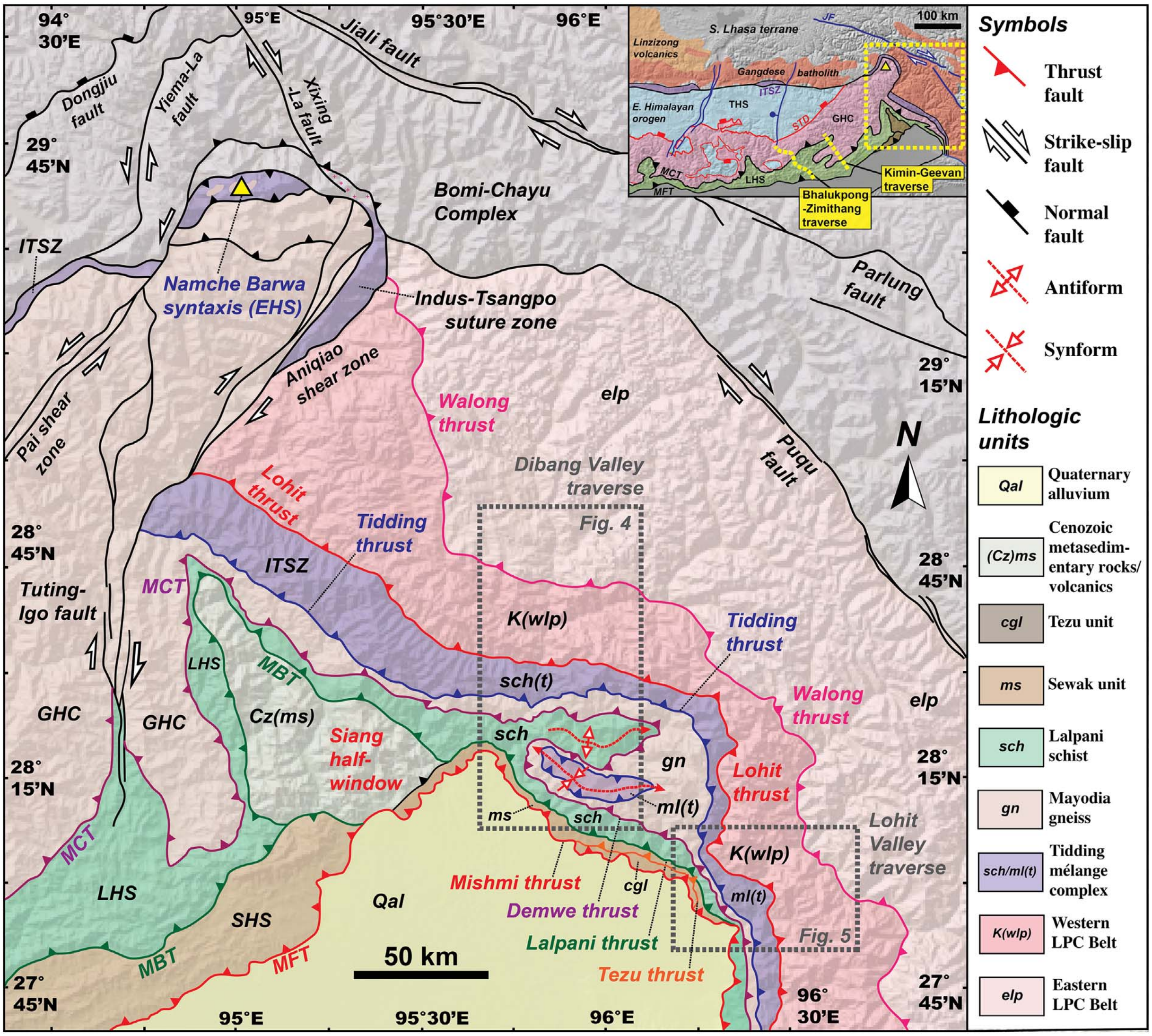

Fig. 3. Geologic map of the easternmost Himalaya and the northern Indo-Burma Ranges compiled from our mapping and that of Ding et al. (2001). Locations of the Dibang Valley (Fig. 4) and Lohit Valley (Fig. 5) traverses are shown in gray boxes. Locations of the Bhalukpong-Zimithang and Kimin-Geevan traverses of Yin et al. (2010a) across the easternmost Himalaya are shown as yellow dashed lines. Index geologic map of the eastern Himalayan orogen is adapted from Webb et al. (2017). Abbreviations: GHC: Greater Himalayan Crystalline complex, ITSZ: Indus-Tsangpo suture zone, JS: Jiali fault, LHS: Lesser Himalayan sequence, MFT: Main Frontal thrust, STD: South Tibetan detachment, and THS: Tethyan Himalayan sequence.

2. Structural geology of the Northern Indo-Burma ranges

The north-trending Indo-Burma Ranges and Central Burma Basin, extending southward from the eastern Himalayan syntaxis to the Andaman Sea, has a linear eastern edge along the right-slip Sagaing fault and a westward convex margin that truncates the west-trending Shillong plateau (Fig. 1) (Mitchell, 1993; Tapponnier et al., 2001; Acharyya, 2010; Yin, 2010). Our study area is located at the northernmost segment of the Indo-Burma Ranges where structures trend northwest, perpendicular to the northeast trend of the eastern Himalayan arc (Figs. 1 and 3). The area exposes drastically different lithologic units, including metasedimentary rocks, mélange complexes, and plutonic rocks, that are bounded by northwest-striking faults (Mitchell, 1993; Gururajan and Choudhuri, 2003; Misra, 2009; Acharyya, 2010). Due to the lack of detailed kinematic studies, the faults in the area have been interpreted as either strike-slip faults accommodating 100′s km of northward indentation of India (e.g., Mitchell, 1993), or northeast-dipping thrusts that are laterally correlative to those of the Himalayan orogen (e.g., the Main Central Thrust) (Gururajan and Choudhuri, 2003; Misra, 2009). To resolve this key issue, we conducted detailed geologic mapping along two deeply-incised river valleys: the north trending Dibang and east trending Lohit Valleys, respectively (Fig. 3). Our work refines the early established tectonostratigraphic framework of previous researchers and provides new constraints on the geometry and kinematics of the major faults in the area.

A total of seven major north- to northeast-dipping thrusts are mapped in the study area (Figs. 3–5). As described below, the strike and slip directions of faults change systematically across the study area: east-striking faults with down-dip stretching lineations occur in the southern region of the study area, whereas northwest-striking faults with down-dip stretching lineations are observed in the northern region of the study area. Structures are shown in cross sections in Fig. 6. The northernmost structure in the map area is the north-dipping Walong thrust of Gururajan and Choudhuri (2003), which places the eastern belt of the Lohit Plutonic Complex (foliated diorite, garnet orthogneiss, migmatite, and marble bands) over the western belt (dominantly foliated Cretaceous diorite suite rocks) (Figs. 4 and 5). The Lohit Plutonic Complex is the eastern extension of the Gangdese batholith in southern Tibet directly north of the Himalaya (Yin and Harrison, 2000; Lin et al., 2013). Along the Dibang Valley traverse (Fig. 4), the Walong thrust is east-striking and north-dipping, placing migmatitic orthogneiss over a foliated diorite intrusive complex that yielded a crystallization age of

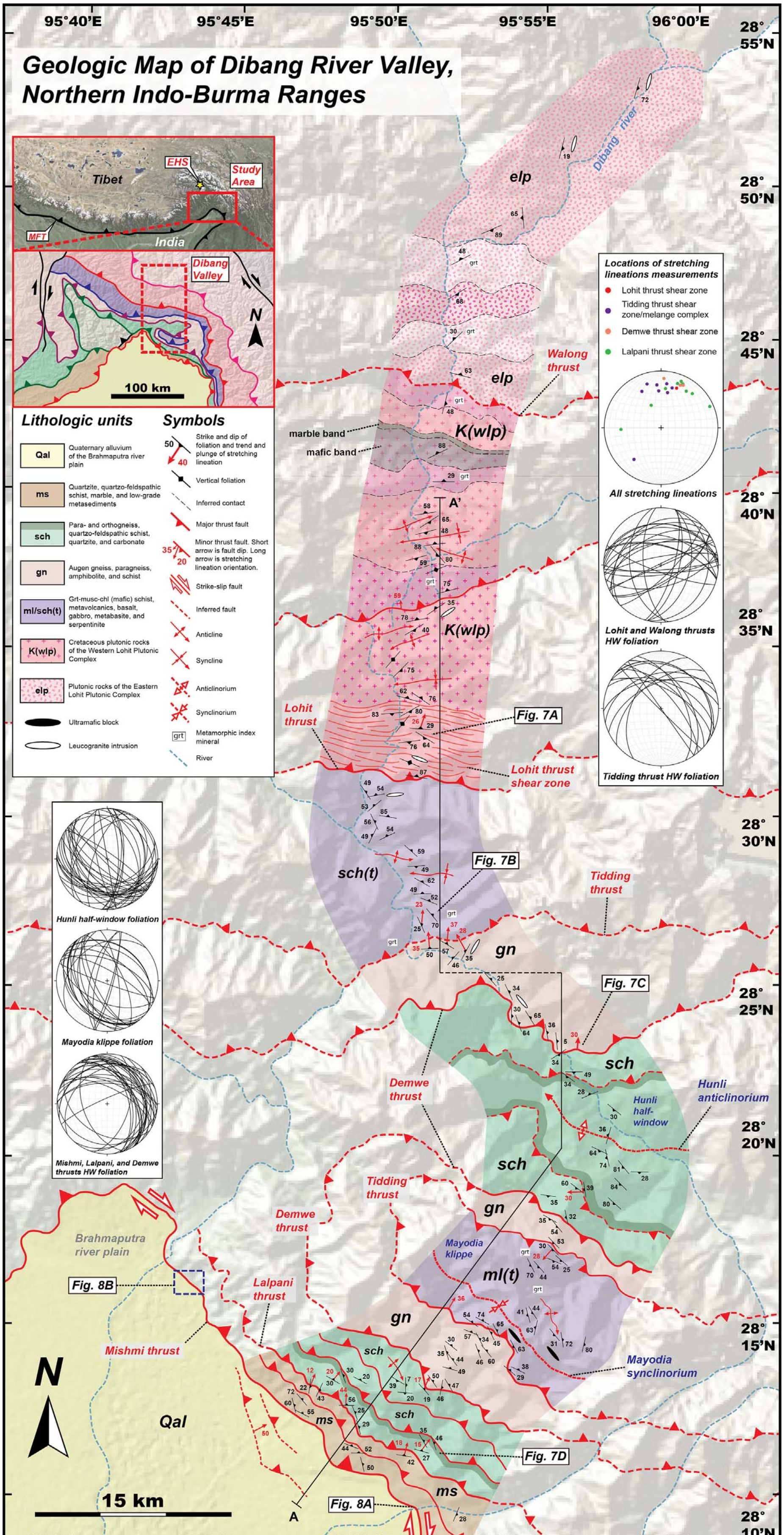

Fig. 4. Geologic map of the Dibang Valley traverse. Abbreviations: EHS: eastern Himalayan syntaxis, HW: hanging wall, MFT: Main Frontal thrust.

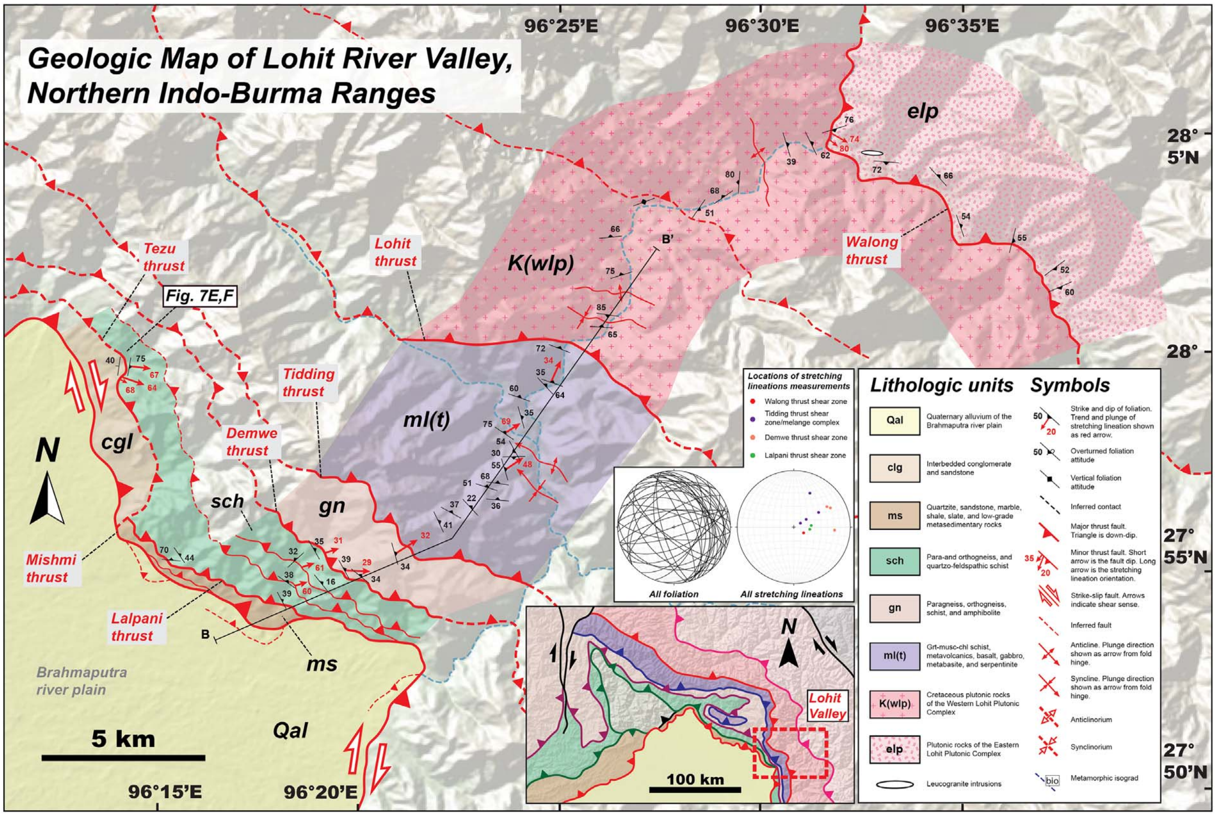

Fig. 5. Geologic map of the Lohit Valley traverse.

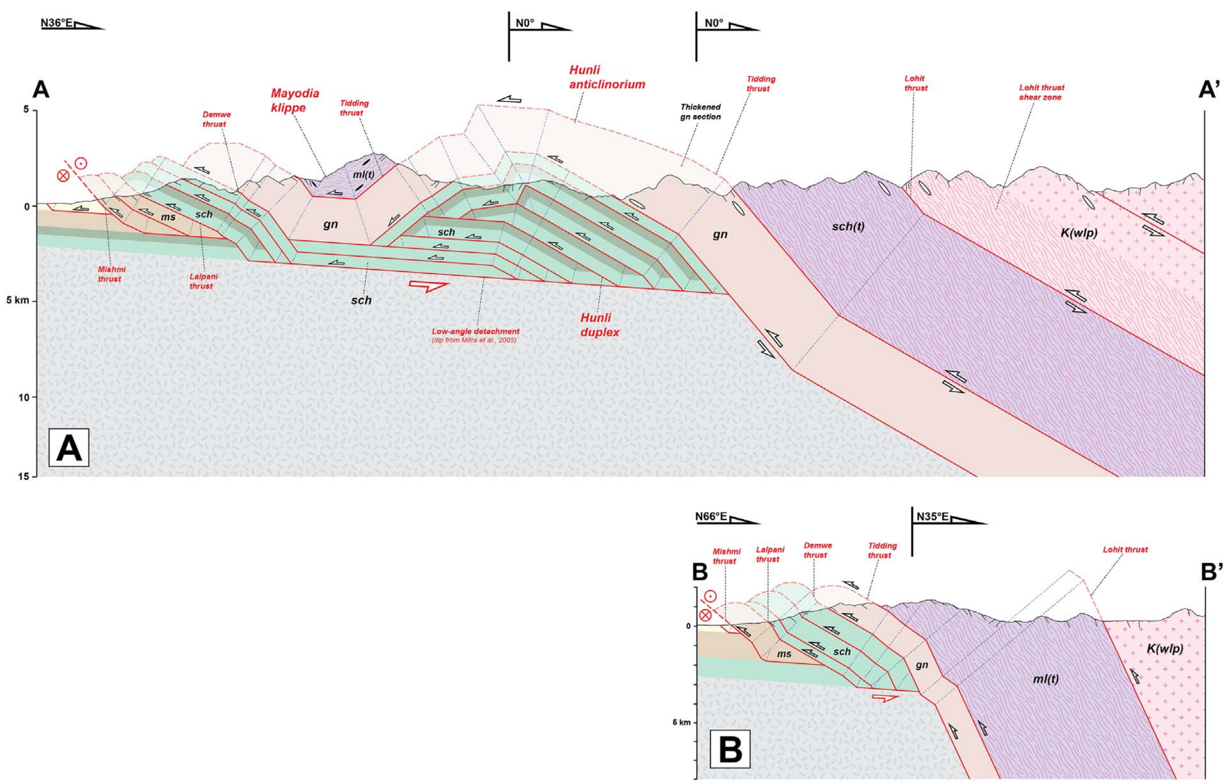

Fig. 6. Cross sections for the (A) Dibang Valley traverse, oriented SW-NE (A-A'), and (B) Lohit Valley traverse, oriented SW-NE (B-B'). See Figs. 4 and 5 for unit descriptions.

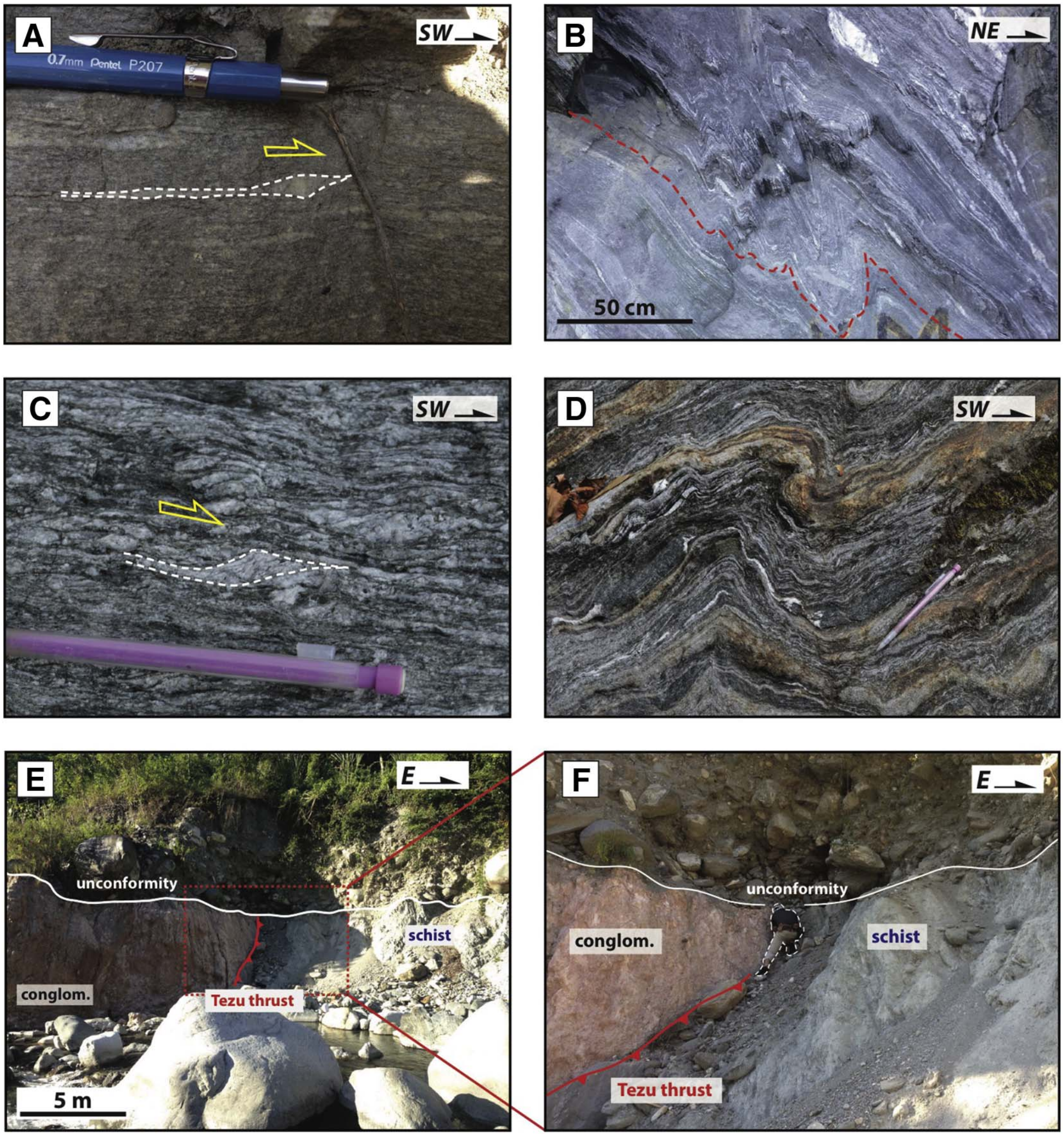

Fig. 7. Outcrop photographs of ductile fabrics within and adjacent to the major thrust shear zones. (A) Foliated diorite displaying asymmetric porphyroclasts indicating top-south shear in the Lohit thrust zone. (B) Chlorite schist containing south-verging tight asymmetric folds within the Tidding thrust shear zone. (C) Augen gneiss displaying asymmetric porphyroclasts and S-C fabric indicating top-southwest shear within the Demwe thrust shear zone. (D) Southwest-verging asymmetric folds in the Lalpani thrust shear zone. (E) and (F) Field relationship of the Tezu thrust placing schist atop conglomerate (conglom.) beds.

~100 Ma (Lin et al., 2013). Along the Lohit traverse, the fault is expressed as a 1-km thick mylonitic shear zone featuring steeply-plunging (> 70°), east-trending stretching lineations (Figs. 4 and 5). S-C fabrics and asymmetric porphyroclasts are well developed in the Walong thrust zone and indicate a top-south sense of shear.

The generally east-striking and north-dipping Lohit thrust of Gururajan and Choudhuri (2003) lies structurally below the Walong thrust (Figs. 4 and 5). This structure places the Lohit Plutonic Complex atop the Tidding mélange complex, which represents the southward continuation of the Indus-Yarlung suture zone in the Indo-Burma Ranges separating Asia in the northeast from India in the southwest (Mitchell, 1993; Yin and Harrison, 2000; Ding et al., 2001; Acharyya, 2010). The Lohit thrust is expressed as a mylonitic shear zone within which foliation is tightly folded with steep dips of 60–80°. Stretching lineations trend to the northeast along both Dibang and Lohit Valleys (Figs. 4 and 5). Asymmetric σ and δ porphyroclasts and S-C fabric indicate top-southwest shear sense (Fig. 7A). Meter-scale leucogranites are also ductily deformed within the Lohit thrust shear zone. The terminations of both the Lohit and Walong thrusts at the left-slip Aniqiao shear zone to the northwest of the study area was mapped from satellite imagery and digital elevation models.

The Tidding mélange complex in the footwall of the Lohit thrust consists of garnet-chlorite schist, metabasite, chert, amphibolite, gabbro, and serpentinized ultramafic rocks. The mélange complex is bounded below by the Tidding thrust with its root zone mapped by Gururajan and Choudhuri (2003) (Figs. 4 and 5). The frontal portion of the Tidding thrust sheet is recognized in our mapping, which is expressed as a flat-lying, mélange-bearing klippe due to folding of the Tidding thrust (Figs. 3 and 4). The ultramafic rocks in the klippe were originally interpreted as the location of the Indus-Tsangpo suture zone (Mitchell, 1993; Acharyya, 2010), but the rootless nature of this lithologic unit and its correlation with the Tidding mélange complex exposed in the root zone of the Tidding thrust reject this early hypothesis. The Tidding thrust in the root zone is characterized by a ~1-km-thick mylonitic shear zone with kinematic indicators such as S-C fabric, asymmetric folds, and rotated porphyroclasts all indicate a top-south sense of shear (Fig. 7B). Stretching lineations within the Tidding thrust shear zone and throughout the Tidding mélange complex trend to the north along Dibang Valley and northeast along Lohit Valley (Figs. 4 and 5). Similar to the structurally higher Lohit thrust zone, meter-scale leucogranites are involved in the ductile deformation along the Tidding thrust zone.

The north-dipping Demwe thrust is a km-scale ductile shear zone juxtaposing the hanging wall unit of paragneiss, augen gneiss, and quartzo-feldspathic schist against the footwall unit of mostly of lower grade schist. Kinematic indicators show a top-south sense of shear (Fig. 7C). Like the overlying Tidding thrust, the Demwe thrust is also folded, which is expressed by an antiform in the north and synform in the south (Fig. 4). The width of the folded thrust sheet is ~20 km in the thrust-transport direction, which constrains its minimum magnitude of slip. Note that the fault trace strikes nearly east-west along the northernmost exposure but the strike changes to a northwest direction along the southernmost exposure (Fig. 4). Stretching lineations trend to the northeast along Dibang Valley and east along Lohit Valley (Figs. 4 and 5).

The northeast-dipping Lalpani thrust of Misra (2009) is expressed as a km-thick shear zone juxtaposing schist in the hanging wall over dominantly phyllite, quartzite, and schist in the footwall. Well-developed mylonitic foliation and north- to northeast-trending stretching lineations are present directly above and below the thrust contact. Stretching lineations within the Lalpani thrust shear zone trend to the north along Dibang Valley and to the east along Lohit Valley (Figs. 4 and 5). Kinematic indicators associated with the mylonitic fabrics, including asymmetric porphyroclasts, asymmetric folds, and S-C fabric indicate top-south to southwest shear (Fig. 7D). The Lalpani thrust and the shear zones at the higher structural levels is that it dips at a much shallower angle of 10–20° rather than mostly > 60° to the north and northeast. In cross section, the Lalpani thrust merges with an inferred decollement at ~3 km depth along both the Dibang (Fig. 6A) and Lohit Valley traverses (Fig. 6B) (Mitra et al., 2005).

The east-dipping Tezu thrust, which is only recognized along the Lohit traverse, strikes north and displays down-dip striation (Fig. 5). The fault is expressed by a meter-thick cataclastic shear zone that juxtaposes metasediments in the hanging wall over a sequence of Tertiary (?) conglomerate and sandstone. The footwall unit is referred here to as the Tezu unit that may be correlative to the Neogene Siwalik Group in the Himalayan foreland basin (Yin, 2006), as the clasts in the conglomerate beds are clearly derived from the nearby thrust sheets mapped in this study. Foliated fault gouge materials in the shear zone display cleavage-defined S-C fabric, which indicate top-west shear (Fig. 7E and F).

The northeast-dipping, range-bounding Mishmi thrust places the Tezu unit over Quaternary deposits (Figs. 3–5, 8A). In addition to the range-bounding thrust, active faults cutting Quaternary sediments are expressed by prominent southwest-facing escarpments within the foreland basin (Figs. 4 and 5). Escarpments are 10′s m in height and 5–10 km in length along strike. The trace of the Mishmi thrust is locally associated with right-lateral stream deflection near Chiddu, which may have resulted from some component of right-slip faulting (Fig. 8B). Based on the sinuous trace of the fault along the range front, the Mishmi thrust appears to be the surface expression of the active, low-angle thrust décollement that serves as the main interface between the Indian plate and upper plate orogenic wedge (Fig. 6), similar to the Main Frontal thrust to the west (Fig. 1). Slip along the décollement triggered the M_W 8.6 1950 Assam earthquake, which has been interpreted to have either strike-slip (Ben-Menahem et al., 1974) or low-angle thrust kinematics (Chen and Molnar, 1977; Coudurier-Curveur et al., 2016).

3. Discussion and conclusions

The most important finding of this work is that the northern Indo-Burma Ranges, directly south of the eastern Himalayan syntaxis, is dominated by dip-slip thrust faults. The only structure that accommodates right-slip deformation is the range-bounding oblique thrust that right laterally displaces active stream channels along its trace (Fig. 8B). Despite local variabilities, our field mapping and systematic

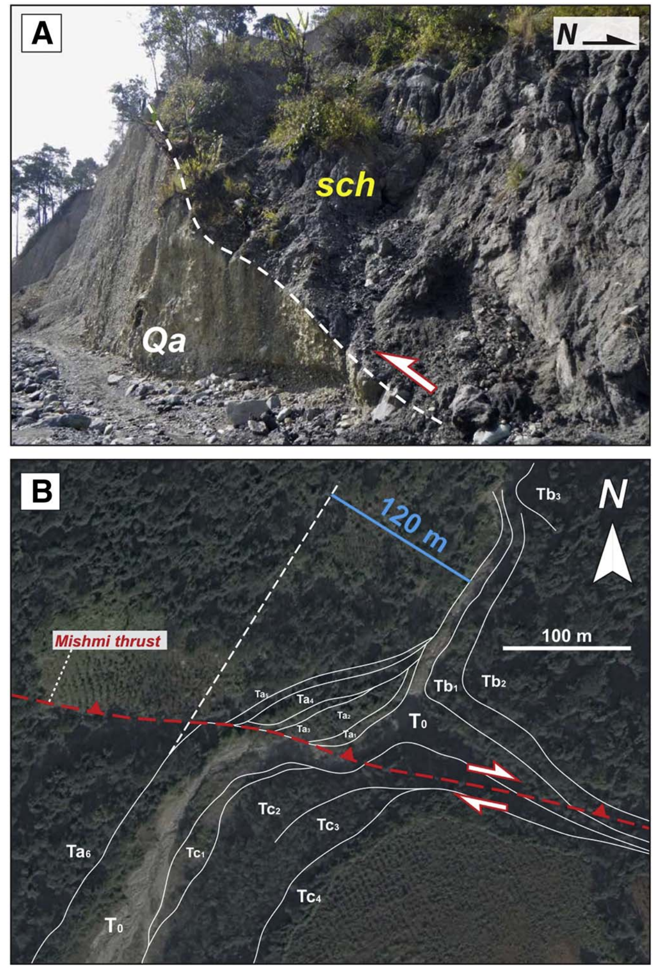

Fig. 8. (A) Outcrop photograph of the Mishmi thrust, placing schist (sch) atop Quaternary conglomerate beds (Qa). (B) Google Earth-based map of cut-and-fill terraces near along the range-bounding Mishmi thrust. Units T_a, T_b, and T_c are fluvial terrace deposits with ages from younger to older. Note that the western edge of the active stream channel is deflected right laterally for ~120 m against the active fault trace, which may result from right-slip motion along the Mishmi fault. See Fig. 4 for location.

documentation of fault kinematic indicators show a clockwise deflection of stretching lineation within the exhumed ductile thrust-shear zones from a nearly north trend in the northern study area to an east trend in the southern study area (Figs. 4 and 5). This southward deflection in lineation trend is evidence for a change in the thrust transport direction along the traces of individual faults. The stretching lineation along the northern segments of all major thrusts has a north to north-northeast trend (Fig. 9C), whereas stretching lineation along the southern segments of the same faults have an east-northeast to east trend (Fig. 9D), a clockwise rotation of almost 90°. This observation is not surprising given that the thrust sheets are non-rigid, expressed by the widespread occurrence of outcrop-scale folds and ductile thrusts (Fig. 7). As a result, the kinematics of thrust shear zones were not related to the motion of rigid blocks, but instead distributed deformation or crustal flow. This explains our observed variable trends of the stretching lineation along the fault traces. A similar example of varying fault kinematics along strike is the active Wenchuan-Yingxiu-Beichuan fault zone bounding the eastern edge of the Tibetan plateau, which displays thrust kinematics in the south and nearly pure right-slip kinematics in the north (Burchfiel et al., 2008).

The varying trend of stretching lineation in our study area mimics the clockwise-rotation pattern of crustal motion detected by the GPS surveys around the eastern Himalayan syntaxis (Zhang et al., 2004; Gan et al., 2007), which was predicted by the crustal-flow model of Cobbold

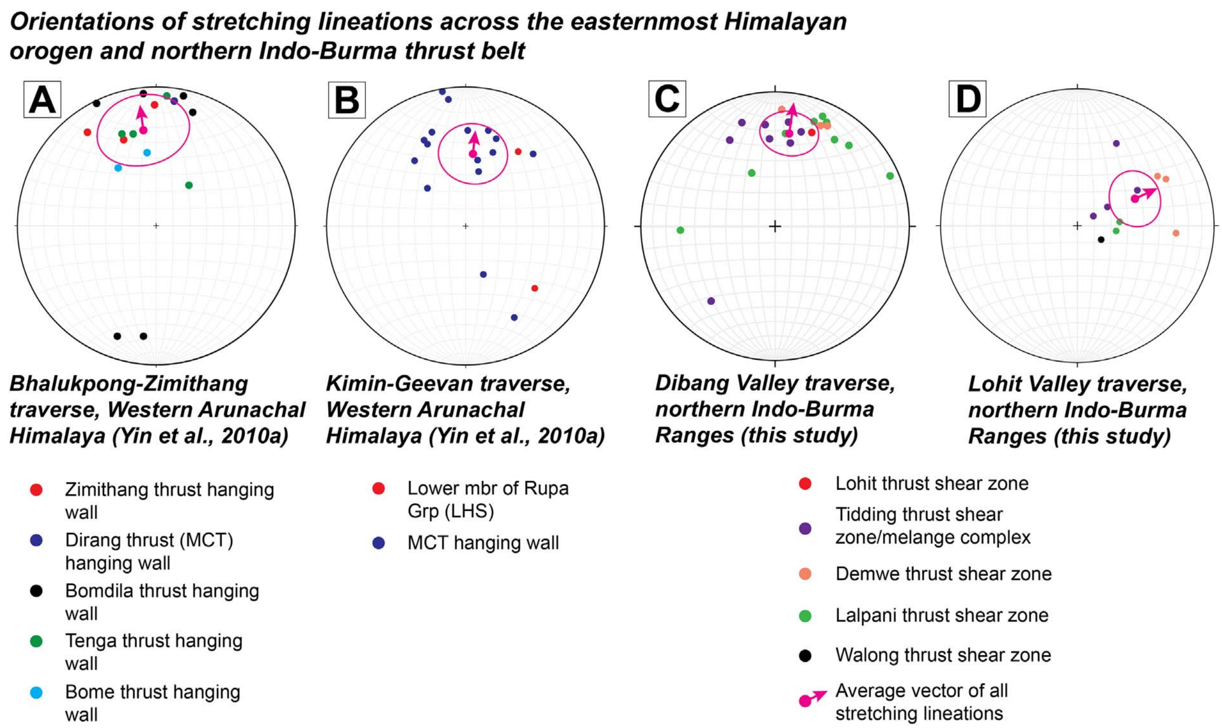

Fig. 9. Stereographic plots of stretching lineation orientations across the easternmost Himalayan orogen and northern Indo-Burma thrust belt (this study), including the (A) Bhalukpong-Zimithang and (B) Kimin-Geevan traverses of Yin et al. (2010a), and (C) Dibang Valley and (D) Lohit Valley traverses of this study.

and Davy (1988) and Royden et al. (1997). The dominance of thrusting across the northernmost Indo-Burma Ranges and varying slip vectors are inconsistent with the right-slip fault-zone model of Mitchell (1993).

The transport direction of thrusts across the northern Indo-Burma Ranges is nearly westward along Lohit Valley (Fig. 9C and D), which is nearly orthogonal to the top-south to top-southeast transport direction of major thrusts across the easternmost Himalayan (Fig. 9A–B) (Yin et al., 2006, 2010a; Burgess et al., 2012; Webb et al., 2013; DeCelles et al., 2016). As the northeast Indian craton is little deformed except along the Oldham and Dauki thrusts bounding the northern and southern margins of the Shillong plateau (Clark and Bilham, 2008; Yin et al., 2010b), the discrepancy in thrust transport directions directly west and south of the eastern Himalayan syntaxis can be attributed to the non-rigid behavior of the overriding Asian plate. Specifically, deformation of overriding-plate lithosphere is best described by distributed shortening approximated by continuum flow. The flow pattern may have been controlled by the combined effects of releasing the gravitational energy potential stored in the thickened Tibetan lithosphere and basal shear caused by westward slab rollback of the Indian oceanic slab below the Indo-Burma Ranges (Ni et al., 1989; Russo, 2012; Rangin et al., 2013).

At this stage of our research, the timing of deformation across the study area is not well constrained. However, the northern Indo-Burma thrust belt features a foreland-ward decrease in deformational fabric temperatures combined with active shortening along the range front, comparable to the style of deformation related to the Cenozoic India-Asia collision across the adjacent easternmost Himalaya. Therefore, the simplest interpretation is that westward younging deformation is consistent with the development of an accretionary fold-thrust belt across the northern Indo-Burma Ranges, as observed along the Himalayan arc (e.g., Ding et al., 2001; Yin et al., 2010a, 2010b; Webb et al., 2013). Although our assertion that the varying trend of stretching lineations supports the crustal flow model may be non-unique, it is the simplest explanation regarding the two competing models in this area: (a) right-slip faulting model of Mitchell (1993) versus (b) the westward thrusting model predicted by the crustal-flow model of Royden et al. (1997).

An important question regarding the spatial deflection of stretching lineation orientations across our study area is whether the trend developed during or after thrusting. In the first case, all thrusts were active simultaneously, but had different transport directions: southward in the north and westward in the south. In the second case, thrust transport in the study area was entirely southward and later distributed right-slip shear resulted in clockwise rotation of the southern part of the thrust belt. Distributed right-slip shear also supports a crustal-flow model, but with different kinematics than predicted by the model of Royden et al. (1997). Note that distributed right-slip shear across the study area is inconsistent with the discrete right-slip faulting model of Mitchell (1993).

The spatial deflection of stretching lineation orientations could also be related to a forward-propagating thrust system in which new thrusts initiate at slight angles to deactivated thrusts towards the front of a radially expanding accretionary complex or around a syntaxis of an orogenic belt (Capitanio and Replumaz, 2013; Moresi et al., 2014). Our field observations favor the simplest interpretation that the trend of stretching lineation is original. If distributed right-slip-shear occurred after the cessation of thrusting, one would expect the development of north-striking strike-slip faults that cut through the ductile thrusts. However, such a cross-cutting relationship was not observed in the study area.

Acknowledgements

This work is supported by grant award #1145038 from the Tectonics Program of the US National Science Foundation. We thank two anonymous reviewers for their detailed comments that improved this manuscript.

References

Acharyya, S.K., 2010. Tectonic evolution of Indo-Burma range with special reference to Naga-Manipur Hills. Geol. Soc. India Mem. 75, 25–43.
Akciz, S., Burchfiel, B.C., Crowley, J.L., Jiyun, Y., Liangzhong, C., 2008. Geometry, kinematics, and regional significance of the Chong Shan shear zone, Eastern Himalayan

Syntaxis, Yunnan, China. Geosphere 4 (1), 292–314.
Avouac, J.P., Tapponnier, P., 1993. Kinematic model of active deformation in central Asia. Geophys. Res. Lett. 20 (10), 895–898.
Ben-Menahem, A., Aboodi, E., Schild, R., 1974. The source of the great Assam earthquake—an interplate wedge motion. Phys. Earth Planet. Inter. 9 (4), 265–289.
Burchfiel, B.C., Royden, L.H., van der Hilst, R.D., Hager, B.H., Chen, Z., King, R.D., Li, C., Lu, J., Yao, H., Kirby, E., 2008. A Geological and Geophysical Context for the Wenchuan Earthquake of 12 May 2008, Sichuan, People's Republic of China, GSA Today. 18. pp. 4–11. http://dx.doi.org/10.1130/GSATG18A.1.
Burgess, W.P., Yin, A., Dubey, C.S., Shen, Z.K., Kelty, T.K., 2012. Holocene shortening across the main frontal thrust zone in the eastern Himalaya. Earth Planet. Sci. Lett. 357, 152–167.
Capitanio, F.A., Replumaz, A., 2013. Subduction and slab breakoff controls on Asian indentation tectonics and Himalayan western syntaxis formation. Geochem. Geophys. Geosyst. 14 (9), 3515–3531.
Chang, L., Flesch, L.M., Wang, C.Y., Ding, Z., 2015. Vertical coherence of deformation in lithosphere in the eastern Himalayan syntaxis using GPS, quaternary fault slip rates, and shear wave splitting data. Geophys. Res. Lett. 42 (14), 5813–5819.
Chen, W.P., Molnar, P., 1977. Seismic moments of major earthquakes and the average rate of slip in central Asia. J. Geophys. Res. Solid Earth 82 (20), 2945–2969.
Clark, M.K., Bilham, R., 2008. Miocene rise of the Shillong Plateau and the beginning of the end for the Eastern Himalaya. Earth Planet. Sci. Lett. 269 (3), 337–351.
Cobbold, P.R., Davy, P.H., 1988. Indentation tectonics in nature and experiment. 2. Central Asia, Bull. Geol. Inst. Univ. 14, 143–162 (Uppsala).
Coudurier-Curveur, A., Kali, E., Tapponnier, P., Karakas, Ç., Ildefonso, S., van der Woerd, J., ... Banerjee, P., 2016. Surface rupture of the 1950 Assam earthquake: active faults and recurrence interval along the Eastern Himalayan syntaxis. In: EGU General Assembly Conference Abstracts. vol. 18. pp. 15794.
DeCelles, P.G., Carrapa, B., Gehrels, G.E., Chakraborty, T., Ghosh, P., 2016. Along-strike continuity of structure, stratigraphy, and kinematic history in the Himalayan thrust belt: the view from Northeastern India. Tectonics 35 (12), 2995–3027.
Ding, L., Zhong, D., Yin, A., Kapp, P., Harrison, T.M., 2001. Cenozoic structural and metamorphic evolution of the eastern Himalayan syntaxis (Namche Barwa). Earth Planet. Sci. Lett. 192 (3), 423–438.
Ding, L., Xu, Q., Yue, Y., Wang, H., Cai, F., Li, S., 2014. The Andean-type Gangdese Mountains: paleoelevation record from the Paleocene-Eocene Linzhou Basin. Earth Planet. Sci. Lett. 392, 250–264. http://dx.doi.org/10.1016/j.epsl.2014.01.045.
Ding, L., Spicer, R.A., Yang, J., Xu, Q., Cai, F., Li, S., Lai, Q., Wang, H., Spicer, T.E.V., Yue, Y., Shukla, A., Srivastava, G., Ali Khan, M., Bera, S., Mehrotra, R., 2017. Quantifying the rise of the Himalaya orogen and implications for the South Asian monsoon. Geology 45 (3), 215–218.
England, P., Houseman, G., 1986. Finite strain calculations of continental deformation: 2. Comparison with the India-Asia collision zone. J. Geophys. Res. Solid Earth 91 (B3), 3664–3676.
England, P., McKenzie, D., 1982. A thin viscous sheet model for continental deformation. Geophys. J. Int. 70 (2), 295–321.
Gan, W., Zhang, P., Shen, Z.K., Niu, Z., Wang, M., Wan, Y., Cheng, J., 2007. Present-day crustal motion within the Tibetan Plateau inferred from GPS measurements. J. Geophys. Res. Solid Earth 112 (B8).
Gururajan, N.S., Choudhuri, B.K., 2003. Geology and tectonic history of the Lohit valley, Eastern Arunachal Pradesh, India. J. Asian Earth Sci. 21 (7), 731–741.
Kornfeld, D., Eckert, S., Appel, E., Ratschbacher, L., Sonntag, B.L., Pfänder, J.A., Ding, L., Liu, D., 2014. Cenozoic clockwise rotation of the Tengchong block, southeastern Tibetan Plateau: a paleomagnetic and geochronologic study. Tectonophysics 628, 105–122.
Leloup, P.H., Arnaud, N., Lacassin, R., Kienast, J.R., Harrison, T.M., Trong, T.T., Replumaz, A., Tapponnier, P., 2001. New constraints on the structure, thermochronology, and timing of the Ailao Shan-Red River shear zone, SE Asia. J. Geophys. Res. Solid Earth 106 (B4), 6683–6732.
Lin, T.H., Chung, S.L., Kumar, A., Wu, F.Y., Chiu, H.Y., Lin, I., 2013. Linking a prolonged Neo-Tethyan magmatic arc in South Asia: Zircon U-Pb and Hf isotopic constraints from the Lohit Batholith, NE India. Terra Nova 25 (6), 453–458.
Maurin, T., Masson, F., Rangin, C., Min, U.T., Collard, P., 2010. First global positioning system results in northern Myanmar: constant and localized slip rate along the Sagaing fault. Geology 38 (7), 591–594.
McKenzie, D., 1972. Active tectonics of the Mediterranean region. Geophys. J. Int. 30 (2), 109–185.
Misra, D.K., 2009. Litho-tectonic sequence and their regional correlation along the Lohit and Dibang valleys, eastern Arunachal Pradesh. J. Geol. Soc. India 73 (2), 213–219.
Mitchell, A.H.G., 1993. Cretaceous–Cenozoic tectonic events in the western Myanmar (Burma)–Assam region. J. Geol. Soc. 150 (6), 1089–1102.
Mitra, S., Priestley, K., Bhattacharyya, A.K., Gaur, V.K., 2005. Crustal structure and earthquake focal depths beneath northeastern India and southern Tibet. Geophys. J. Int. 160 (1), 227–248.
Moresi, L., Betts, P.G., Miller, M.S., Cayley, R.A., 2014. Dynamics of continental accretion. Nature 508 (7495), 245–248.
Ni, J.F., Guzman-Speziale, M., Bevis, M., Holt, W.E., Wallace, T.C., Seager, W.R., 1989. Accretionary tectonics of Burma and the three-dimensional geometry of the Burma subduction zone. Geology 17 (1), 68–71.
Rangin, C., Maurin, T., Masson, F., 2013. Combined effects of Eurasia/Sunda oblique convergence and East-Tibetan crustal flow on the active tectonics of Burma. J. Asian Earth Sci. 76, 185–194.
Royden, L.H., Burchfiel, B.C., King, R.W., Wang, E., Chen, Z., Shen, F., Liu, Y., 1997. Surface deformation and lower crustal flow in eastern Tibet. Science 276 (5313), 788–790.
Russo, R.M., 2012. Source-side shear-wave splitting and upper-mantle flow beneath the Arakan slab, India-Asia-Sundalind triple junction. Geosphere 8 (1), 158–178.
Ryan, W.B., Carbotte, S.M., Coplan, J.O., O'Hara, S., Melkonian, A., Arko, R., Bonczkowski, J., 2009. Global multi-resolution topography synthesis. Geochem. Geophys. Geosyst. 10 (3).
Tapponnier, P., Peltzer, G., Armijo, R., 1986. On the mechanics of the collision between India and Asia. Geol. Soc. Lond., Spec. Publ. 19 (1), 113–157.
Tapponnier, P., Zhiqin, X., Roger, F., Meyer, B., Arnaud, N., Wittlinger, G., Jingsui, Y., 2001. Oblique stepwise rise and growth of the Tibet Plateau. Science 294 (5547), 1671–1677.
Taylor, M., Yin, A., 2009. Active structures of the Himalayan-Tibetan orogen and their relationships to earthquake distribution, contemporary strain field, and Cenozoic volcanism. Geosphere 5 (3), 199–214.
Wang, E., Burchfiel, B.C., 1997. Interpretation of Cenozoic tectonics in the right-lateral accommodation zone between the Ailao Shan shear zone and the eastern Himalayan syntaxis. Int. Geol. Rev. 39 (3), 191–219.
Wang, E., Burchfiel, B.C., Royden, L.H., Chen, Z., Chen, J., 1998. Late Cenozoic Xiangshuihe-Xiaojiang, Red River, and Dali fault systems of southwestern Sichuan and central Yunnan, China. Geol. Soc. Am. Spec. Pap. 327, 1–108.
Webb, A.A.G., Yin, A., Dubey, C.S., 2013. U-Pb zircon geochronology of major lithologic units in the eastern Himalaya: implications for the origin and assembly of Himalayan rocks. Geol. Soc. Am. Bull. 125 (3–4), 499–522.
Webb, A.A.G., Guo, H., Clift, P.D., Husson, L., Müller, T., Costantino, D., ... Wang, Q., 2017. The Himalaya in 3D: slab dynamics controlled mountain building and monsoon intensification. Lithosphere L636–1.
Yin, A., 2006. Cenozoic tectonic evolution of the Himalayan orogen as constrained by along-strike variation of structural geometry, exhumation history, and foreland sedimentation. Earth Sci. Rev. 76 (1), 1–131.
Yin, A., 2010. Cenozoic tectonic evolution of Asia: a preliminary synthesis. Tectonophysics 488 (1), 293–325.
Yin, A., Harrison, T.M., 2000. Geologic evolution of the Himalayan-Tibetan orogen. Annu. Rev. Earth Planet. Sci. 28 (1), 211–280.
Yin, A., Dubey, C.S., Kelty, T.K., Gehrels, G.E., Chou, C.Y., Grove, M., Lovera, O., 2006. Structural evolution of the Arunachal Himalaya and implications for asymmetric development of the Himalayan orogen. Curr. Sci. 195–206.
Yin, A., Dubey, C.S., Kelty, T.K., Webb, A.A.G., Harrison, T.M., Chou, C.Y., Célérier, J., 2010a. Geologic correlation of the Himalayan orogen and Indian craton: part 2. Structural geology, geochronology, and tectonic evolution of the Eastern Himalaya. Geol. Soc. Am. Bull. B26461–1.
Yin, A., Dubey, C.S., Webb, A.A.G., Kelty, T.K., Grove, M., Gehrels, G.E., Burgess, W.P., 2010b. Geologic correlation of the Himalayan orogen and Indian craton: part 1. Structural geology, U-Pb zircon geochronology, and tectonic evolution of the Shillong Plateau and its neighboring regions in NE India. Geol. Soc. Am. Bull. 122 (3–4), 336–359.
Zhang, P.Z., Shen, Z., Wang, M., Gan, W., Bürgmann, R., Molnar, P., Wang, Q., Niu, Z., Sun, J., Wu, J., Hanrong, S., 2004. Continuous deformation of the Tibetan Plateau from global positioning system data. Geology 32 (9), 809–812.